

Mechanical and durability properties of recycled aggregate concrete with ternary binder system and optimized mix proportion

O. E. Babalola¹, P. O. Awoyera^{2*}, M. T. Tran¹, D-H Le¹, O. B. Olalusi³, A. Vilorio^{4,5}
and D. Ovallos-Gazabon⁶

¹Faculty of Civil Engineering, Ton Duc Thang University, Ho Chi Minh City, Vietnam

²Department of Civil Engineering, Covenant University, Ota, Nigeria

³Discipline of Civil Engineering, University of KwaZulu-Natal, Durban, South Africa

⁴Universidad de la Costa, Barranquilla, Colombia

⁵Universidad peruana de ciencias aplicadas, lima, peru

⁶Universidad Simon Bolivar, Barranquilla, Colombia

*Corresponding author's email: awopaul2002@gmailcom

Abstract

This study aimed to investigate the mechanical and durability properties of recycled aggregate concrete with a ternary binder system and optimized mix proportion. Two concrete batches were developed using a densified mix design approach (DMDA) to evaluate the required mix proportions. Batch I have GGBS content varied at 0%, 10%, 20%, 30%, 40% and 50% at constant w/b ratio of 0.45, while batch II concrete mix have varied water/binder ratios: 0.3, 0.35, 0.4, 0.45 and 0.5 at constant GGBS replacement level of 30%. The fine aggregate (river sand) of the two batches was blended with fly ash at optimum loose packing density (FA + Sand) and superplasticizer (SP) was incorporated in the mix at a constant level of 1.4%. A control mix, comprising of natural aggregate was also developed. The results obtained showcased the feasibility of producing structural concrete with recycled aggregates using GGBS and fly ash. The mechanical and durability properties were best at 30% GGBS content and 0.35 water/binder ratio. The DMDA for mix proportion adopted for RAC contributed significantly to improving its **properties when compared to NAC, especially** at the optimum observed RAC mix with compressive strength of 52 MPa. Also, the mix demonstrated good permeability resistance in terms of chloride-ion ingress and capillary water absorption.

keywords: recycled aggregate concrete; densified mix design; ternary binder, durability; mechanical properties

1.0 Introduction

Concrete is a versatile building and construction material that will continue to be in demand far into the future, thus, meaning that a world without concrete is hard to imagine [1]. As a composite material, concrete is made up of different constituents which include binding materials such as cement and supplementary cementitious materials, aggregates and water [2,3]. The aggregates comprise of 75 percent of concrete by volume including fine grade particles up to 4.75 mm and coarse grade particles up to 20 mm in size [4].

Recycling C&D wastes for usage in concrete production is now an important issue in fostering sustainable development, products of recycled C&D has been considered as recycled concrete aggregates in concrete production [5-9]. RCA differs from natural aggregates (NA) due to old attached cement mortal, which causes higher porosity, water absorption, and lower strength and negatively affects the durability and mechanical properties of fresh and hardened concrete [10]. Dimitriou, Savva, & Petrou [11] attributed significant reduction in strength loss and improvement of chloride resistance of RAC to the treatment of RCA by removing old attached mortal and addition of mineral admixtures such as fly ash at 25% and silica fume at 5% replacement level for ordinary Portland cement (OPC) in RAC conventional concrete mix. However, observed slow strength development at 28 days was attributed to the slow pozzolanic reaction of fly ash. Recycled materials and some (industrial and agricultural) waste materials are suitable for blending with OPC as a substitute or partial replacement for binders in concrete production, fly ash, GGBS and silica fumes are three well-known examples of cement replacement materials that are in use today [1]. British Standard BS8500 [12] has defined a maximum masonry/fines content of 5%, maximum lightweight material/asphalt content of 0.5%, and maximum other foreign materials content of 1% for RCA.

Supplementary materials blended with cement influence properties of RAC for chloride resistance properties; its effects were considered significant [13–15]. RCPT test conducted by Obla et al [16] revealed for concrete containing slag and fly ash at a given w/c ratio, the charges passed in coulombs decreases with an increase in slag and fly ash content as higher charge indicate higher chloride ion penetrability. Kou and Poon [17] obtained a decrease of total porosity of RAC at 25%

fly ash replacement level; however, increased porosity was observed at 35% replacement level, this was attributed to the dilution effect of cement and thus the formation of fewer products of hydration at an initial stage. Furthermore, the experimental results of Obla et al [16] show that initial and final setting times of concrete mix containing slag and fly ash decreases with an increase in cement content at each w/c ratio considered, attributing this to the effect of HRWRA used. Another important concern in RAC is its high water capacity potential which has posed serious concern to its durability properties especially in harsh environment usage, in such cases, RAC performs poorly in comparison to NAC [18–20].

An attempt has been made to overcome RAC shortcomings using various mix proportions and recycled aggregate replacement levels, adjustment to the cement content of RAC mixes was used to produce RAC with equivalent or sometimes greater resistance to chloride. Generally, high cement content in the concrete mix requires higher water content that can cause detrimental effect such as segregation and bleeding [21]. Some researchers have considered a reduction of w/b ratio to obtain higher strength in RAC, this, however, has resulted to a large amount of cement in the mixing process that may cause drying shrinkage and creeping [22]. Drying shrinkage and creep of concrete made with recycled aggregates are up to 100% higher than concrete with a corresponding conventional aggregate due to the presence of old mortar [23]. Peng et al. [24] also observed different main type of flaws for RAC at low and high w/b ratio, the treatment process for removal of attached mortar caused decrease in compressive strength and fracture energy for RAC with low w/b ratio 0.255 caused increase of the same properties in RAC with high w/b ratio 0.586.

In general, positive results have been recorded with different supplementary cementitious materials in RAC and conventional mix. However, the problem of concrete shrinkage and creeping occur in such mixtures as a result of increase in cement content and a low w/b ratio to improved strength and durability of RAC. Few studies are available regarding approach to solving this problem; hence, the need to investigate behavior of densely packed aggregates (Fly ash + sand) + RCA as constituent for RAC mix with minimum paste volume of cement blended with GGBS and study the influence of varying w/b ratio while focusing on enhancing its durability and strength properties. This paper adopted DMDA mix proportions [25] to achieve best engineering properties for RAC through densely packed constituent materials and optimum cement paste volume. The influence of mix proportion obtained for conventional mix and densified mix design algorithms (DMDA) was targeted in this experimental work by comparing RAC mix to a conventional control

mix of natural aggregates. Laboratory tests for determining physical properties, including water absorption capacity, specific gravity, porosity, and the residual mortar content (RMC) was carried out on coarse recycled aggregate based on relevant ASTM specifications. The results demonstrated the feasibility of producing structural concrete with optimum recycled aggregate mix proportion and ternary binder system with FA as filler with OPC, and GGBS as supplementary cementitious material, while also determining its influence on the durability and mechanical properties of the mixture.

2. Experimental Program

2.1. Material

The materials used for this experimental program for the production of recycled aggregate concrete are binder (OPC and GGBS and FA), recycled coarse aggregate, natural fine and coarse aggregates, water, and superplasticizer.

2.1.1 Binder Material

Binder consists of ordinary Portland cement (OPC) Type I Portland cement general-purpose cement based on BS 12 [26] classification and type F Waste fly ash conforming to ASTM C 618[27], and with Blaine's fineness of 4000 g/cm², fineness in terms of specific surface area between 250 and 550 m²/kg and specific gravity of 2.3 g/cm³. GGBS was obtained from Ho Chi Minh, Vietnam. Table 1 gives the chemical and physical properties of the cementitious replacement materials. A Sulphonated Naphthalene formaldehyde type superplasticizer (CERAPLAST 300) was used for the mix.

2.1.2 Aggregates

Recycled aggregates (RA) were sourced from a site of the demolished building structure of around 20 years in Ho Chi Minh City, the demolished concrete collected was further crushed using a small jaw crusher to obtain aggregates in its unscreened and ungraded state and pass through mechanical sieves. Minor impurities were removed and fine RCA of particle size passing through sieve 4.75 mm and coarse RCA of particle sizes ranging from 4.75 - 25 mm was obtained. **This experimental study did not consider the use of fine recycled aggregates.** For the natural aggregates, coarse aggregates of crushed granite aggregates of carbonaceous mineral type with particle size ranging

from 4.75 - 25 mm were sourced from the quarry, while river sand was used as fine aggregates. Fig 1 shows the sieve analysis curve for the fine aggregate, while the characterization testing of the physical properties of aggregates is presented in Table 2.

Table 1. Chemical composition and physical properties of FA and GBFS

Chemical Composition (%)	FA type F	GBFS
SiO ₂	53	17.8
Al ₂ O ₃	25.8	11.6
Fe ₂ O ₃	6.5	25.8
CaO	9.5	33.5
Mg O	0.7	4
Na ₂ O	0.3	0.1
K ₂ O	3.8	-
SO ₃	0.4	0.3
TiO ₂	-	0.4
Physical composition		
Fineness (blaine) m ² /kg	295	400
Loose dry unit weight kg/m ³	650	
Specific gravity	2.3	
Retaining on 45 um sieve (%)	8.2	

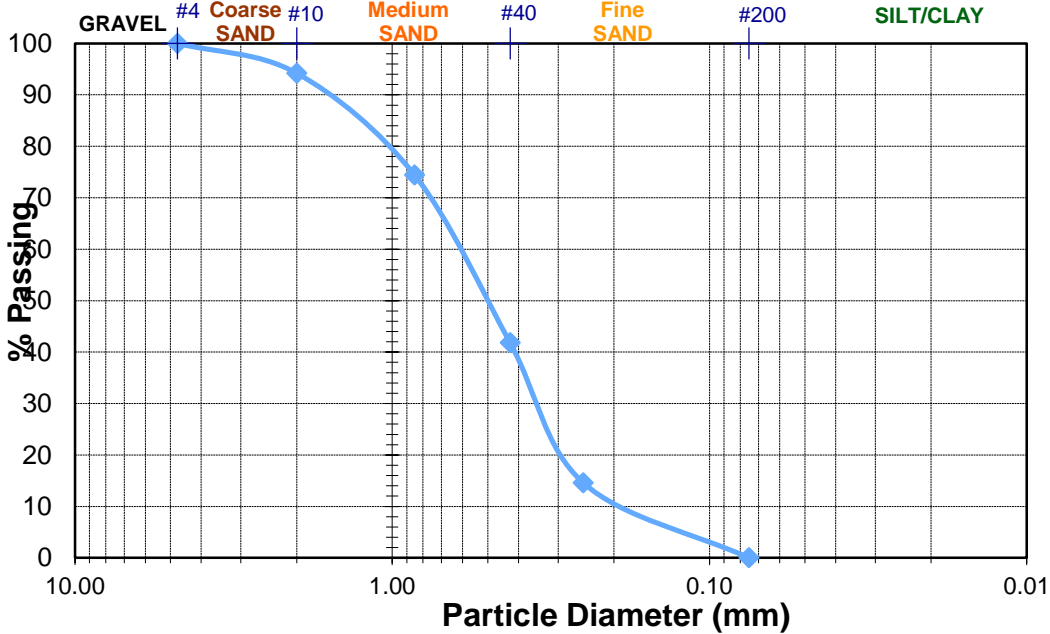


Fig 1: Particle size distribution of river sand used in this study.

Table 2. Physical properties for coarse and fine aggregates.

Aggregate	Absorption capacity (%)	Porosity (%)	Specific gravity	Los Abrasion value (%)	Bulk density (kg/m ³)
RCA	5.2	12.75	2.35	34	1490
NCA	1.25	4.25	2.6	22.3	1515
River Sand	0.9		2.65		1550

2.2 Mix proportions and testing of variables

The mix proportion was done in two groups. A mix proportion was made for produce normal concrete (NC), while the DMDA was adopted for recycled aggregate concrete (RAC) mix with the ternary binding system. FA was used as filler for natural sand at optimum loose packing density followed by a mixture of (Sand + FA) with RA to obtain optimum packing density (Figs. 2 a & b). In other to investigate the influence of mix proportions and supplementary materials on RAC properties, this experimental work considered two concrete mix batch group, batch I, and batch II. GGBS was used to replace OPC at varying percentage level from 0%, 10%, 20%, 30% 40% and 50% at constant cement w/b ratio in batch I concrete mix while for batch II concrete mix, aggregates constituent remains constant with GGBS replacement level fixed at 30% and varying w/b ratio range of 0.3, 0.35, 0.4, 0.45, and 0.5 were adopted. The main idea of the DMDA was to ensure that enhanced performance RAC when the bulk density of the concrete mixture is highest. The binder paste volume was fixed at $N = 1.2$ and constant water reducing agent of 1.4% was used for all concrete mix. Mix nomenclature and proportion used is as presented in Table 3. The method followed Hwang [25]'s findings, as summarized here:

an approach to optimizing mix design for properties of RAC was based on the properties of basic materials constituents of RAC using a densified mix design approach (DMDA) suggested by Chang [21]. The optimal amount of fly ash to fill aggregate voids is determined; then, the coarse aggregate was added to the mixture in proportion to the obtained optimum packing density of (sand + Fly ash) + RCA. The ratio of fly ash to both fine and coarse aggregates of the maximum unit weight was used to calculate the void volume (V_v). When cement paste content equals to void volume $V_p = NV_v$, where N is magnification factor for paste volume taking as constant of 1.2 in this experiment, with this all the void space is entirely filled with cement paste. Summary of the procedure is given as:

- (i) Different trials of mix prepared by filling the fine aggregate with varying percentage of ash (FA + GBFS) to obtain the optimum amount of ash + fine aggregates as shown in Figure 2.0 (a)

- (ii) Different trial mixes of mixture for (Fly ash + Fine aggregate) amount to fill the voids in coarse aggregates to achieved optimum packing density and porosity ratio as shown in Figure 2.0 (b)
- (iii) Constant ‘ α ’, ‘ β ’ through optimum weights of materials obtained during laboratory experiments was determined with equation 1 and 2

$$\alpha = \frac{W_{\text{fly}}}{W_{\text{fly}} + W_s} \quad (1)$$

$$\beta = \frac{W_s + W_{\text{fly}}}{(W_s + W_{\text{fly}}) + W_{\text{ca}}} \quad (2)$$

$$\xi = \frac{W_{\text{slag}}}{W_{\text{slag}} + C} \quad (3)$$

Where

- W_{fly} : weight of fly ash (kg/m^3 of concrete);
 W_s : weight of fine aggregate (kg/m^3 of concrete);
 W_{ca} : weight of coarse aggregate (kg/m^3 of concrete);
 W_{slag} : weight of blast-furnace slag (kg/m^3 of concrete); and
 C : weight of cement (kg/m^3 of concrete).

The least volume of void is determined using

$$V_v = 1 - \sum \left(\frac{W_i}{\gamma_i} \right)$$

Determine the least volume of lubricating paste needed V_p

$$n \cdot V_v = V_p$$

where n is a multiplier for lubricating paste

$$V_s = 1 - V_p$$

V_p = Volume of Paste

V_s = Volume of solids (ash+fine sand + coarse aggregate)

The mix proportion of each gradient is calculated as follows:

$$W_s = \frac{V_{agg}}{\left(\frac{\alpha}{1-\alpha}\right) \frac{1}{\gamma_{fly}} + \frac{1}{\gamma_s} + \left(\frac{1-\beta}{\beta-\alpha\beta}\right) \frac{1}{\gamma_{ca}}} \quad (4)$$

$$W_{ca} = W_s \cdot \frac{(1-\beta)}{(\beta-\alpha\beta)} \quad (5)$$

$$W_{fly} = W_s \cdot \left(\frac{\alpha}{1-\alpha}\right) \quad (6)$$

$$C = \frac{V_p - \frac{\lambda W_{fly}}{\lambda_w}}{\left[\frac{\lambda}{\gamma_w} + \frac{1}{\gamma_c} + \left(\frac{\xi}{1-\xi}\right) \left(\frac{\lambda}{\gamma_w} + \frac{1}{\gamma_{sl}}\right)\right]} \quad (7)$$

Where γ is the specific gravity of the material, and the suffices w, c, sl, fly, s, ca, refer to water, cement, slag, fly ash, sand, and crushed stone, respectively.

With water to the cementitious material ratio (λ), the weight of water is

$$W = (C + P) \cdot \lambda \quad (8)$$

$$W_{sl} = \xi/(1 - \xi) \cdot C \quad (9)$$

Finally, the water-to-solid ratio is defined as:

$$W/S = W/(C+P+W_{ca}+W_s) \dots\dots\dots 10$$

Chang (2004) also used it to optimize the design mix for high-performance concrete with varying water/solid ratio as it was considered a significant parameter in the concrete mix design.

The testing items and standards conducted on RAC for this study in its fresh and hardened state are presented in Table 4. Slump and air content of fresh RAC were measured, the mechanical properties such as compressive strength, tensile strength, and modulus of elasticity of hardened RAC as well as performance to chloride-ion penetration and capillary water absorption were also considered to evaluate its durability performance.

Table 3. Mix proportion for natural and recycled aggregate concrete mixtures developed for this experiment

S/N	Mix ID	% GB		% W/S	Fine aggregate (kg/m ³)			OPC (kg/m ³)	GGBS (kg/m ³)	FA (kg/m ³)	WATER (kg/m ³)	% SP
		FS	W/B		Coarse aggregates (kg/m ³)							
					Natural	RCA	NCA					
1	N0-45	0	0.45	9.9	532		990	433	0	0	195	0.8
2	D0-45	0	0.45	5.9	770	115	0	160	0	127	130	0.8
3	D10-45	10	0.45	5.9	770	115	0	144	16	127	129	0.8
4	D20-45	20	0.45	5.9	770	1115	0	127	32	127	127	0.8
5	D30-45	30	0.45	5.9	770	1115	0	111	47	127	128	0.8
6	D40-45	40	0.45	5.9	770	1115	0	94	63	127	128	0.8
6	D50-45	50	0.45	5.9	770	1115	0	78	78	127	128	0.8
7	D30-30	30	0.3	4.7	770	1115	0	158	68	127	105	0.8
8	D30-35	30	0.35	5.2	770	1115	0	140	60	127	114	0.8
9	D30-40	30	0.4	5.6	770	1115	0	124	53	127	122	0.8
10	D30-45	30	0.45	5.9	770	1115	0	111	47	127	128	0.8
11	D30-50	30	0.5	6.2	770	1115	0	99	42	127	133	0.8

Remark: 1. Mix no: Da-b, a is GGBS content (%); b is w/cm ratio; respectively. 2. Mix no: D represents the densified mixture design algorithm (DMDA), Mix no: N represents ACI 211.1-81 standard practice for selecting proportions for Normal heavyweight, and mass concrete

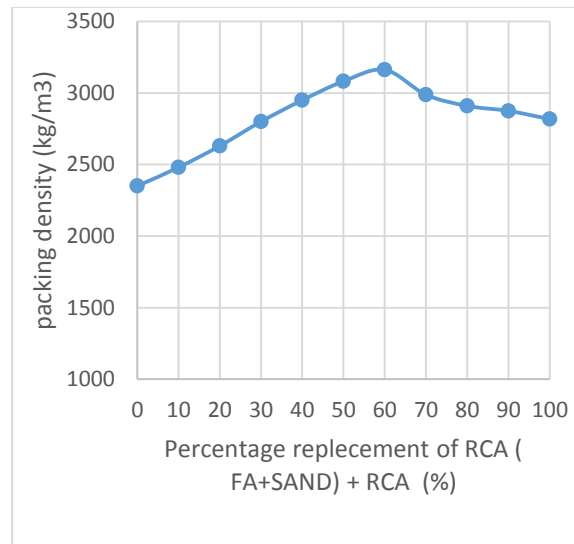
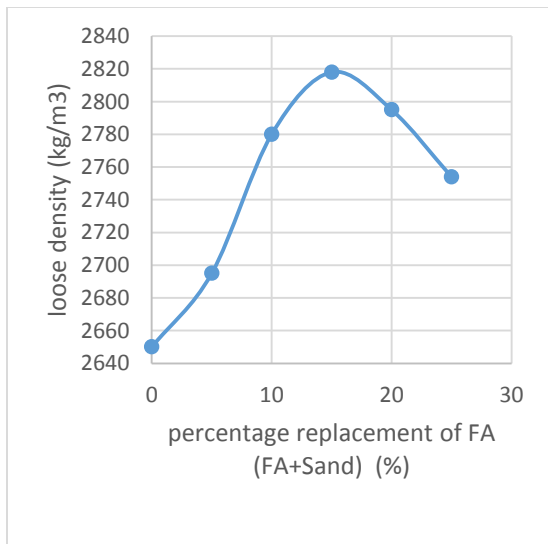


Figure 2: (a) loose density (FA + Sand)

(b) Packing density of (FA + Sand) + RCA

2.3 Test methods

Concrete constituent materials were mixed in a mechanical mixer. The details of the tests performed on both fresh and hardened concrete is presented in Table 4. Eleven numbers of different concrete mix were produced; fresh concrete mixed was tested for slump (C143), air content and density (C138) ASTM standards. All specimens were standard cured following ASTM C192 in a moist room at $73\pm 3^{\circ}\text{F}$ immediately after casting the specimens for the duration before testing. Cylindrical specimen size of 100 x 200 mm was cast and tested for compressive strength and split tensile strength following C39 and C 496, respectively at 7, 28, and 90 days. A total number of 99 cylindrical concrete specimens of size $\emptyset 100 \times 200$ mm was tested using a universal testing machine (UTM) at a loading rate of 2.4 kN/s (540 lb/s), The maximum load and maximum compressive stress recorded. The compressive strength value presented for each concrete mix type was obtained by taking the average of three specimens of the same curing period. Tensile strength of specimen was determined at 7, 28, and 90 days curing regimes.

A rapid indication of different specimen's resistance to the penetration of chloride ion was determined through rapid chloride penetration test (RCPT) following ASTM C1202 [28]. Cylindrical concrete of 100 x 200 mm dimension was sliced at the top side to obtain concrete disks of size 100 x 50 mm, a 60 V DC power source current was passed through the concrete specimen for 6hrs and the resistance of the concrete specimen to chloride ions penetration was evaluated by the total charge passed. A solution of 3% NaCl and 0.3 M NaOH was placed in anode and cathode acrylic cells, respectively.

The rate of absorption (sorptivity) of water by different specimens was determined by measuring the increase in the mass of specimens resulting from the absorption of water as a function of time as per ASTM C1585[29]. The bottom surface of the concrete specimen was exposed to water ingress by capillary suction, while the other surface was sealed with epoxy resin. In preparation for the test, concrete disc of size 100 mm diameter with 50 mm thickness were cut from the middle part of the 200 mm long cylinder to ensure good representative of sample of concrete quality and minimum variation; specimens were placed in a desiccator oven at temperature $50 \pm 2^{\circ}\text{C}$ and RH $80 \pm 3\%$ for 3 days. Mass gain due to sorption was measured at definite intervals for the first six hours. The density of wet mix concrete with varying mix proportion was determined according to ASTM C34. All the mixtures were consolidated using rodding and tapping the side of the container

with a rubber mallet repeated for three (3) layers. The top of the container was leveled off and the weight was measured using a scale.

Table 4. details of specimen for fresh and hardened test

No	Test (testing ages)	Items	Sample dimension (mm)	Quantity of sample	Standards
<i>fresh properties</i>					
1	Slump	-	-	-	ASTM C 143[30]
2	Air content & Fresh density	-	-	-	ASTM C 138[31]
3	Setting times (initial and final)	-	-	-	ASTM C 191[32]
<i>Hardened properties</i>					
4	Compressive Strength	-	Ø100x200 mm	78	ASTM C 39[33]
5	RCPT	-	Ø100x200 mm	26	ASTM C 1202[28]
6	Sorptivity	-	Ø100x50 mm	26	ASTM C 1585[29]
7	Split Tensile strength	-	Ø100x200 mm	78	ASTM C 496[34]

3 Results and Discussions

3.1 Slump and entrapped air content

The slump and fresh density of control and RAC mix were determined as shown in Figure 3, with addition of superplasticizer being kept constant at 0.8%. The slump for control mix was 125 mm. However, in the modified mixtures, the slump increased with increase in GGBS replacement level in the range of 78 mm – 114 mm from 0 % to 50%, respectively. This shows improved workability with GGBS addition, and it could be attributed to the spherical and glass texture of the particle surface. This result is consistent with the previous report on GGBS [35,36]. Increased content of GGBS in the mixture practically makes it acts as lubricant in RAC mix [37]. The slump of concrete mixtures having 35% FA and 55% GGBS was higher than the control mixtures (zero mineral admixture). Similarly, in batch II mixture, w/b ratio increased slump in RAC from 50 mm in w/b ratio 0.3 to 110 for w/b ratio of 0.5. At a constant GGBS replacement level of 30%, there was a slight reduction in slump as the w/b ratio increased due to DMDA adopted, and this, however, has slightly contributed to low increase in slump observed with increase w/b ratio. The lubricating effect of GGBS was observed with a slump reduction of 38% and 14% in D0-45 without GGBS

admixture and D30-45 with 30% GGBS content, respectively.

Air content reduction of 44% was observed in RAC concrete without GGBS admixture (D0-45) when compared to the control mixture (N0-45), shown in Table 5. This was due to the dense concrete matrix of DMDA in RAC that compensated for the porous adhered mortar in RA. In Figure 4, it can be seen that an increase in GGBS content in the RAC caused further reduction of 6%, 24% and 57%, 64% and 71% in air content for D10, D20 and D30, D40 and D50 mix, respectively, at a constant w/b ratio 0.45 compared to D0-45 mix without GGBS. This was expected because the addition of mineral admixtures generally allows less air to be entrapped in the concrete due to more filling of air voids in concrete [38].

3.2 Fresh density

The fresh density of concrete in the plastic state was also determined; Figure 5 shows the correlation between fresh density, air content, and GGBS replacement level. The least void percentage compensated the detrimental effect of porous nature of old adhered mortar on RAC fresh density in packing of aggregates with DMDA, a slight reduction in fresh density of 5.1% was RAC in D0-45 comparing to control conventional mix N0-45 with natural aggregate. Increase in GGBS replacement content has slight influence increase in fresh density with RAC density ranging from 2230 – 2348 kg/m³, which is similar to control mix (2350 kg/m³) with only minimal fresh density loss of 5.1% - 0.1% for 10% – 50% GGBS content respectively. This could arise due to reduced air void in RAC as GGBS increase. Table 5 shows a slight fresh increase in fresh density as the w/b ratio decreases from 0.5 to 0.30, which was attributed to a reduction in the water content from 133 to 105 kg/m³ resulting in the denser concrete mix. The same trend was observed by Kou and Poon [39] in self-compacting concrete made with 100% RA, where reduction of water content in w/b ratio from 0.44 – 0.35 led to a slight increase in fresh mixture density.

Table 5. Results of fresh concrete properties for slump, air content density properties

S/N	Mix ID	Slump (mm)	Air content (%)	Fresh density (kg/m ³)
1	N0-45	125	5.2	2350
2	D0-45	78	3.6	2230
3	D10-45	83	3.4	2278
4	D20-45	95	2.9	2285
5	D30-45	108	2.3	2340

6	D40-45	110	2.2	2343
6	D50-45	114	2.1	2348
7	D30-30	50	1.5	2368
8	D30-35	72	1.8	2350
9	D30-40	85	2.0	2343
10	D30-45	108	2.3	2340
11	D30-50	110	2.8	2333

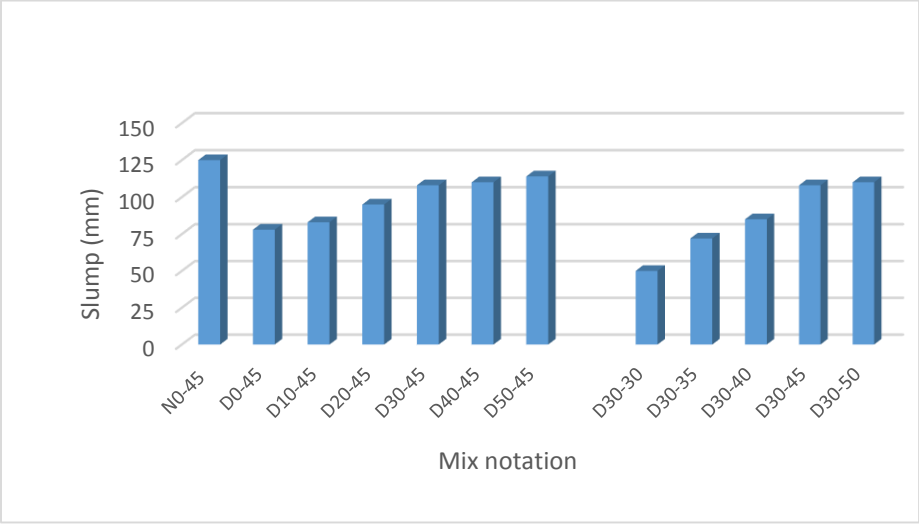


Figure 3: Slump of control and RAC mix

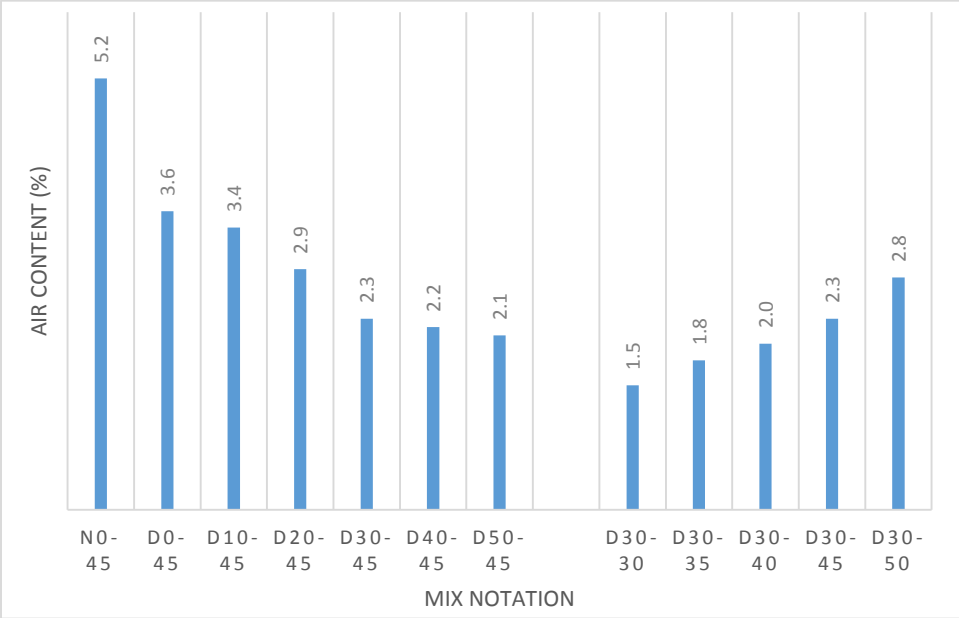


Figure 4: Air content of variation in control and RAC mix

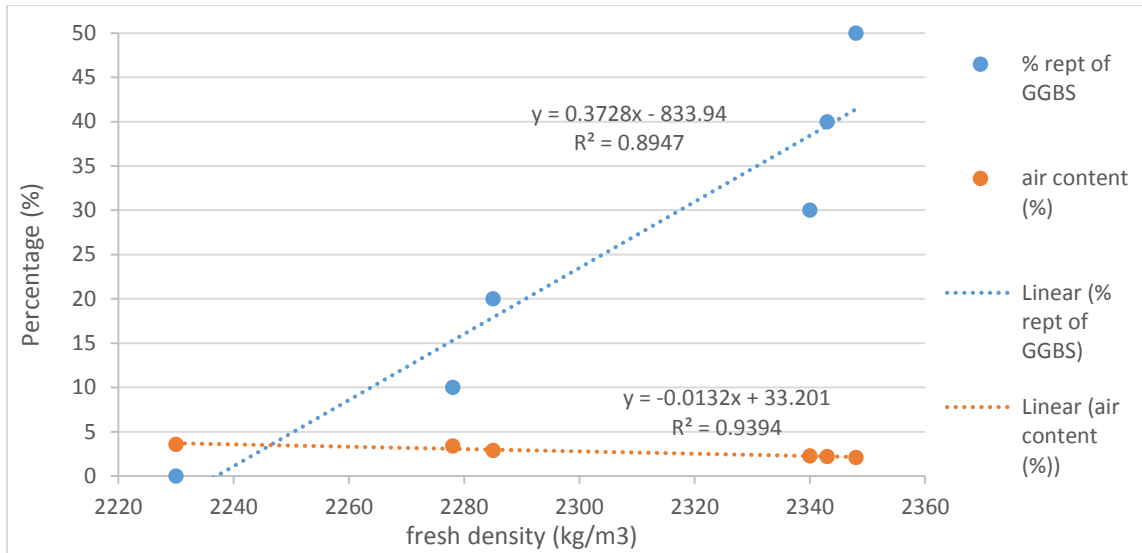


Figure 5. Correction between air content, GGBS replacement content and fresh density of RAC mixtures

3.3 Compressive strength

The compressive strength test performed on hardened RAC specimens after curing at 7, 28 and 90 according to ASTM C-39 specifications. Fig. 6 shows the compressive strength of the two concrete mix batches I and II with % GGBS replacement level and w/b ratios. Delay early strength development was observed as GGBS content increases at 7 days in all concrete mixes. The slow pozzolanic reaction of GGBS was considered the main responsible factor. GGBS mortars and concretes attained compressive strength at slow rate than OPC under normal curing environments [40], [41] similarly observed compressive strength decreased gradually with the augmentation of slag content at early stage while with wet cured concrete GGBS at 50% and 60% substitution positively influence compressive strength beyond the control concrete. However, after 7 days, strength gain increases in RAC considerably over the control mix because of the continuous reaction of calcium hydroxide produced from the hydration of Portland cement, hence, increased strength rate development with specimen age. Concrete mix D40-45 and D30-30 attained the highest compressive strength of 30% and 35.3% more than control conventional mix in batches I and II, respectively at 28 days. (Suda & Rao, 2020) observed at 28 days in mix TC6 containing (OPC60%+MS10%+GGBS30%) highest value of 17.67% more than control concrete mix with conventional mix design. It was further observed that compressive strength of RAC with GGBS

continue to increase in all concrete mix with age, comparing 90 days and 28 days strength, D20-45 has highest increased strength rate of 22.3% in batch I, D30-30 (27.3%) in batch II, for mix without GGBS, D0-45 (17.6%) and N0-45(16%). D30-30 has the highest compressive strength showing a low water /binder ratio with optimum quality paste develop high strength in RAC higher than the conventional AC design normal aggregate concrete. Compressive strength value at 7, 28 and 90 days is presented in Table 6

Table 6. Mechanical properties of RAC Mixtures

Mix Group	Mix notation	Compressive Strength (MPa)			Tensile Strength (MPa)		
		7 days	28 days	90 days	7 days	28 days	90 days
Batch I	N0-45	22	30.6	35.5	1.70	2.80	2.97
	D0-45	21	31.7	37.3	1.80	3.00	3.13
	D10-45	19.6	33.5	40.5	1.80	3.20	3.43
	D20-45	19.2	35.8	43.8	1.90	3.50	3.70
	D30-45	18.5	37	44	1.94	3.52	4.02
	D40-45	18	39.8	45.6	2.10	3.70	4.22
	D50-45	15	39.2	42.2	2.10	3.91	4.20
Batch II	D30-30	20	41.4	52.7	2.10	3.82	4.65
	D30-35	20	38	48	2.00	3.74	4.62
	D30-40	19.3	37.4	46.8	2.00	3.68	4.12
	D30-45	18.3	37	44	1.94	3.52	4.02
	D30-50	16.35	33	41.5	1.75	3.28	3.83

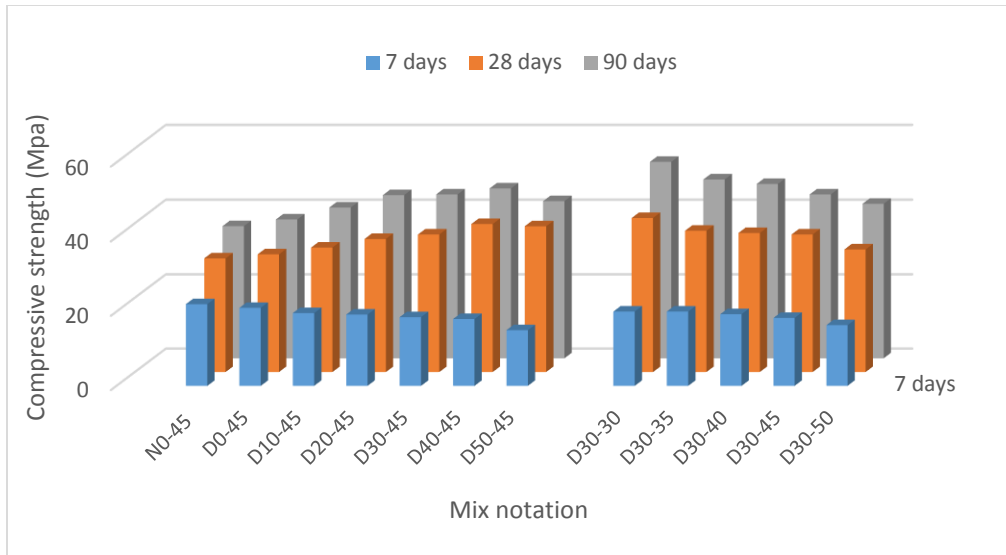


Figure 6: Compressive strength of the two concrete batches I and II with % GGBS replacement level and w/b ratios.

3.4 Splitting tensile strength:

Figure 7 shows the splitting tensile strength of all concrete mix type. A similar trend compared to compressive strength was observed. The tensile strength of the specimen for the control mix at 7, 28, and 90 days was 1.8 MPa, 3.0MPa, and 3.13MPa, respectively. From Table 6, comparing tensile strength of D0-45 (without GGBS) compared to N0-45 (natural aggregate) control conventional mix, increased tensile strength of 7% and 10% was observed at 7 days and 28 days respectively. This increase in strength could be as a result of enhanced bond strength at the ITZ as a result of the greater surface area of RA in contact with the new cementitious matrix in RAC [43–47]. Nevertheless, the DMDA mix approach used for RAC also contributed positively to the development of tensile strength resulting in dense packing and bonding of aggregates. Pradhan et al. [48] obtained a similar increase in tensile strength of 6.3% in RAC using particle packing method (PPM) compared to IS: 10262 code 2009 mix, no reason was, however, given for this observation. for the batch I, at constant w/b ratio with DMDA mix, tensile strength was also observed to increase with GGBS content, the dense sand + fly ash and GGBS resulted in RAC with finer pores and denser structure, thus improving the interface strength. A significant increase in tensile strength of 8% and 26% was observed at 10% and 50% GGBS replacement, respectively. Berndt [49] observed a similar trend of 20% Split tensile strength increase at 50% GGBS replacement level; however, he recorded no additional tensile strength gain at 70% GGBS addition.

For split tensile strength result in batch II, similar trend compared to compressive strength was observed, decrease w/b ratio enhanced the effectiveness of GGBS to tensile strength gain of RAC ranging from 3.48, 3.52, 3.68, 3.74 and 3.82 at w/b 0.5, 0.45, 0.40, 0.30 and 0.3 respectively at 28 days. However, a minimal improvement was seen comparing 28 days and 90 days tensile strength gain.

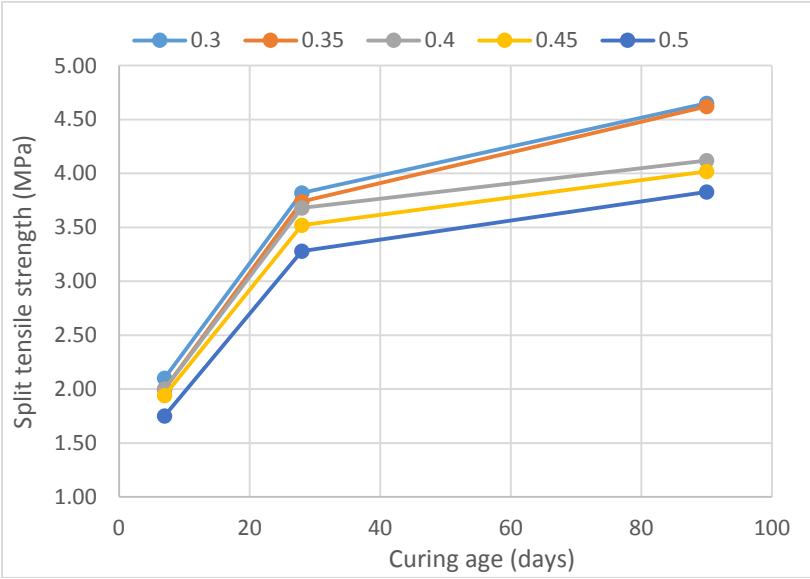
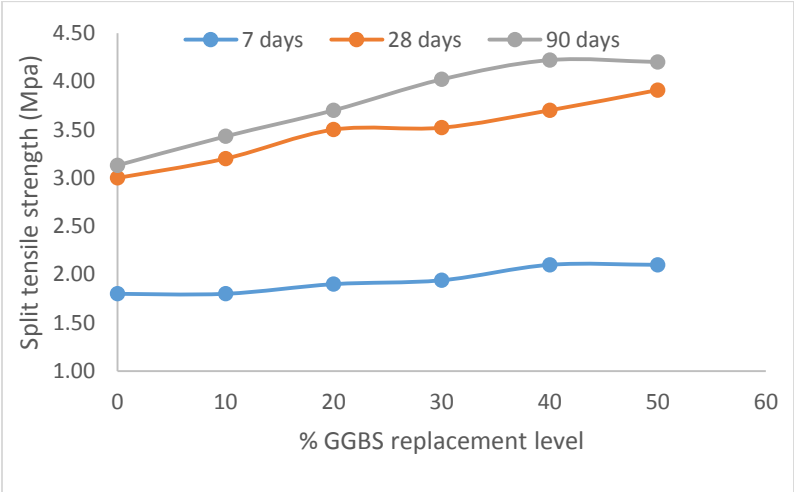
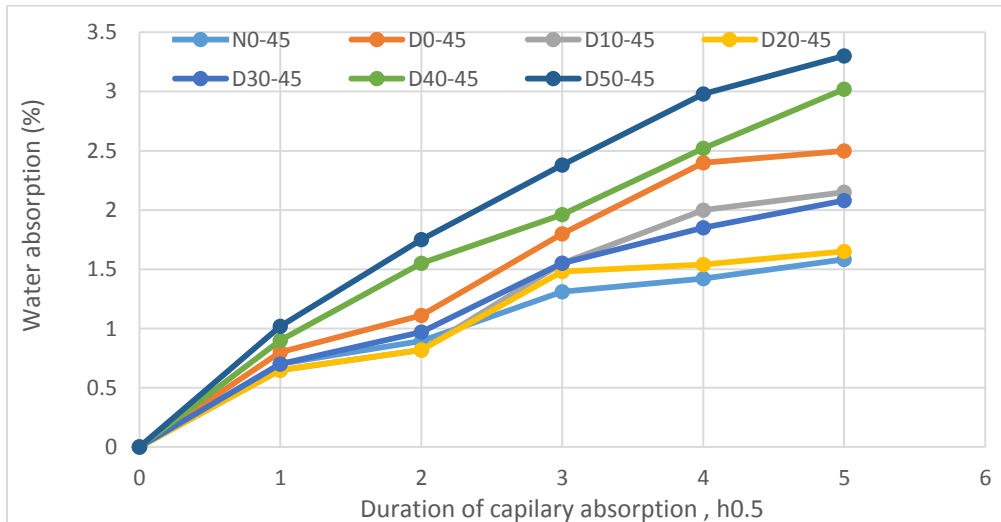


Figure 7. (a) Tensile strength of RAC at varying GGBS replacement level (b) tensile strength of varying w/b ratio with age

3.5 Water absorption by capillary action

The transport of liquids into porous solids due to surface tension acting in capillaries is sorptivity [50] water absorption of all RAC and NC control mix was determined at 28 and 90 days (Fig. 8). 21% increase in total water absorption was observed for N0-45 (0.43) control and D0-45 (0.52) concrete mix respectively at 28 days. Dodds [19] observed 48.78% increase in sorption coefficient corresponding to 0.41 (0% RA) and 0.61 (100% RA) with CEM I concrete at 24 hours test. The higher water absorption capacity of RC aggregates was due to the presence of old adhered mortar with high porosity that creates a path for water flow in RAC [51] observed improvement in this study was attributed to close particle packing and less void in RAC mixes. For the GGBS replacement level in Batch I concrete, Figure 7(a) shows lower water absorption with an increase in GGBS up to 20% replacement level. This was attributed to a pozzolanic reaction producing secondary C-S-H gel and refine pore structures [52–54]. The inclusion of GGBS reduced the sorption coefficients at 24 hours [19], however higher water absorption was noticed in higher GGBS replacement percentage as a result of increase porosity arising from dilution effect of cement that hinders the formation of hydration products. **Figures 8 a & b show** water/binder ratio has a significant influence on water absorption in batch II concrete, w/b ratio is directly proportional to water absorption. Guo et al. (2018) gave strong negative impact for increased w/c ratio on RAC.



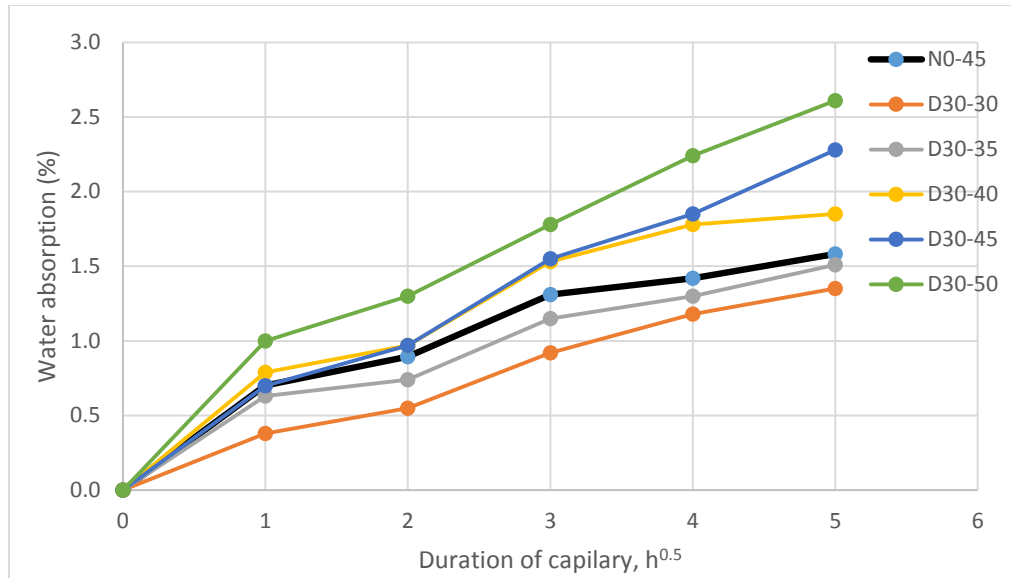


Figure 8: (a) Water absorption with varying GGBS replacement level (b) Water Absorption at varying w/b ratio at 28 days

3.6 Chloride-ion penetration

Figure 9 shows the chloride-ion penetration in the mixtures. The total charge passed through D0-45 (RAC without GGBS) was 5350 coulombs and 4500 coulombs at 28 days and 90 days, respectively. This showed the influence of fly ash as filler on the dense matrix structure achieved through DMDA mix. Higher charge passed measured was as a result of detrimental effect of higher porosity of adhered mortar in RA [55]. Moreover, high alumina content in fly ash triggers pozzolanic reactions, thus, resulting in the formation of greater and denser calcium silicate hydrate(CSH) structure and C3A. So, increase in alumina content caused reduction in total charge in the RAC [56]. In the batch I mix, improved chloride resistance was seen with an increase in GGBS content in RAC. This result corroborates the findings of the following authors [57–59]. Concrete with 50% GGBS replacement D50-45 has the lowest total charge passed with 62% and 64% reduction compared to the NC control mix at 28 days and 90 days, respectively. Faella et al. [60] reported a similar lower total charge passed in RAC with an addition of 30% GGBS having a 56% reduction after 28 days. Furthermore, reduction of chloride ion penetration was observed in all concrete mix with increasing curing age. This was because of continued hydration reactions of cement with mineral admixtures that further reduce the porosity and pore connectivity of concrete [61,62]. For batch II, Increasing the water/binder ratio resulted in decreasing in the diffusion

coefficient of chloride ion because the increased w/b ratio increases the pore content of concrete [63]. There was 40% reduction in total charge passed in D30-30 with w/b ratio 0.3 compared to D30-50 with w/b ratio 0.5

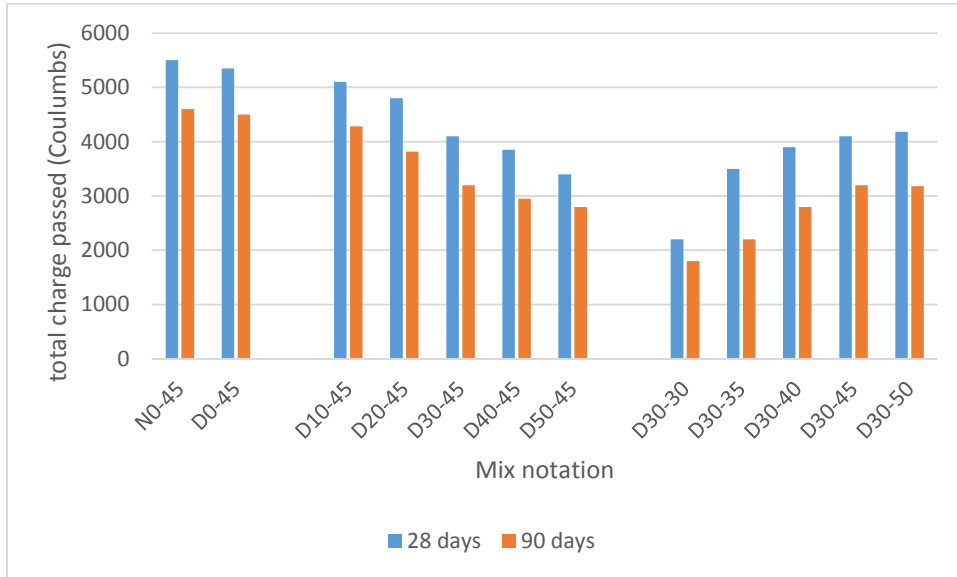


Figure 9. Influence of GGBS content on the total charge passed of recycled aggregate concrete

4. Conclusion

The need to optimize the use of routinely discarded materials for the development of sustainable product units cannot be overemphasized. This study investigated the mechanical and durability properties of recycled aggregate concrete following the ternary binder system and optimized mix proportion. The following conclusions were drawn from the study:

1. The addition of superplasticizer at a constant rate of 0.8% yielded a slump of 125 mm for the control mix, but overall, slump increased with increasing GGBS content. In this context, the slump was in the range of 78 mm – 114 mm for mixtures having GGBS between 0 % to 50%.
2. Early strength development in the concrete mixture was slow as the GGBS content increases at 7 days, which was attributed to the slow pozzolanic reaction of GGBS. Concrete mix D40-45 and D30- 30 attained the highest compressive strength of 30% and 35.3% more than control conventional mix in batches I

and II at 28 days, respectively.

3. The mix that had 30% GGBS demonstrated good permeability resistance in terms of chloride-ion ingress and capillary water absorption.

Conflicts of interest

The authors declare no conflicts of interest.

References

- [1] M.S. Imbabi, C. Carrigan, S. McKenna, Trends and developments in green cement and concrete technology, *Int. J. Sustain. Built Environ.* 1 (2012) 194–216.
doi:<https://doi.org/10.1016/j.ijbsbe.2013.05.001>.
- [2] M. Behera, S.K. Bhattacharyya, A.K. Minocha, R. Deoliya, S. Maiti, Recycled aggregate from C&D waste & its use in concrete—A breakthrough towards sustainability in construction sector: A review, *Constr. Build. Mater.* 68 (2014) 501–516.
- [3] O.E. Babalola, P.O. Awoyera, Suitability of <i>Cordia millenii</i> Ash Blended Cement in Concrete Production, *Int. J. Eng. Res. Africa.* 22 (2016) 59–67.
doi:10.4028/www.scientific.net/JERA.22.59.
- [4] M. Moini, The optimization of concrete mixtures for use in highway applications, (2015).
- [5] C.-C. Fan, R. Huang, H. Hwang, S.-J. Chao, Properties of concrete incorporating fine recycled aggregates from crushed concrete wastes, *Constr. Build. Mater.* 112 (2016) 708–715. doi:10.1016/j.conbuildmat.2016.02.154.
- [6] S. Karthik, P.R.M. Rao, P.O. Awoyera, Strength properties of bamboo and steel reinforced concrete containing manufactured sand and mineral admixtures, *J. King Saud Univ. - Eng. Sci.* (2017). doi:10.1016/j.jksues.2016.12.003.
- [7] P. Awoyera, R. Gobinath, S. Haripriya, P. Kulandaisami, New Light Weight Mortar for Structural Application: Assessment of Porosity, Strength and Morphology Properties, in: S.C. Satapathy, K.S. Raju, K. Molugaram, A. Krishnaiah, G.A. Tsihrintzis (Eds.), *Int. Conf. Emerg. Trends Eng.*, Springer International Publishing, Cham, 2020: pp. 59–65.
- [8] P.O. Awoyera, J.M. Ndambuki, J.O. Akinmusuru, D.O. Omole, Characterization of

- ceramic waste aggregate concrete, HBRC J. (2016).
doi:<https://doi.org/10.1016/j.hbrcj.2016.11.003>.
- [9] P. Murthi, P. Awoyera, P. Selvaraj, D. Dharsana, R. Gobinath, Using silica mineral waste as aggregate in a green high strength concrete: workability, strength, failure mode, and morphology assessment, *Aust. J. Civ. Eng.* (2018). doi:10.1080/14488353.2018.1472539.
- [10] C. Shi, Y. Li, J. Zhang, W. Li, L. Chong, Z. Xie, Performance enhancement of recycled concrete aggregate – A review, *J. Clean. Prod.* 112 (2016) 466–472.
doi:<https://doi.org/10.1016/j.jclepro.2015.08.057>.
- [11] G. Dimitriou, P. Savva, M.F. Petrou, Enhancing mechanical and durability properties of recycled aggregate concrete, *Constr. Build. Mater.* 158 (2018) 228–235.
doi:<https://doi.org/10.1016/j.conbuildmat.2017.09.137>.
- [12] B.S. British Standard, 8500, Concrete–Part 1: Complementary British Standard to BS EN 206-Part 1: Method of Specifying and Guidance for the Specifier, Br. Stand. Institution, London. (2006).
- [13] R. Corral-Higuera, S.P. Arredondo-Rea, M.A. Neri-Flores, J.M. Gomez-Soberon, J.L. Almaral-Sanchez, A. Castorena-Gonzalez, J H Martinez-Villafane, F. Almeraya-Calderon, Chloride ion penetrability and corrosion behavior of steel in concrete with sustainability characteristics., *Int. J. Electrochem. Sci.* 6 (2011) 958–970.
- [14] R.V. Silva, J. de Brito, R. Neves, R. Dhir, Prediction of Chloride Ion Penetration of Recycled Aggregate Concrete, *Mater. Res.* 18 (2015) 427–440.
http://www.scielo.br/scielo.php?script=sci_arttext&pid=S1516-14392015000200427&nrm=iso.
- [15] N. Singh, S.P. Singh, Carbonation resistance and microstructural analysis of Low and High Volume Fly Ash Self Compacting Concrete containing Recycled Concrete Aggregates, *Constr. Build. Mater.* 127 (2016) 828–842.
doi:<https://doi.org/10.1016/j.conbuildmat.2016.10.067>.
- [16] K. Obla, C. Lobo, R. Hong, H. Kim, Optimizing Concrete Mixtures for Performance and Sustainability, in: *Int. Concr. Sustain. Conf. Seattle*, 2012.
- [17] K. Shicong, C.S. Poon, Compressive strength, pore size distribution and chloride-ion penetration of recycled aggregate concrete incorporating class-F fly ash, *J. Wuhan Univ. Technol. Sci. Ed.* 21 (2006) 130–136. doi:10.1007/BF02841223.

- [18] B. Mas, A. Cladera, T. del Olmo, F. Pitarch, Influence of the amount of mixed recycled aggregates on the properties of concrete for non-structural use, *Constr. Build. Mater.* 27 (2012) 612–622. doi:<https://doi.org/10.1016/j.conbuildmat.2011.06.073>.
- [19] W. Dodds, C. Goodier, C. Christodoulou, S. Austin, D. Dunne, Durability performance of sustainable structural concrete: Effect of coarse crushed concrete aggregate on microstructure and water ingress, *Constr. Build. Mater.* 145 (2017) 183–195.
- [20] C. Medina, W. Zhu, T. Howind, M.I.S. de Rojas, M. Frías, Influence of mixed recycled aggregate on the physical – mechanical properties of recycled concrete, *J. Clean. Prod.* 68 (2014) 216–225. doi:<https://doi.org/10.1016/j.jclepro.2014.01.002>.
- [21] P.-K. Chang, W.-M. Hou, A study on the hydration properties of high performance slag concrete analyzed by SRA, *Cem. Concr. Res.* 33 (2003) 183–189.
- [22] P.K. Chang, An approach to optimizing mix design for properties of high-performance concrete, *Cem. Concr. Res.* 34 (2004) 623–629. doi:[10.1016/j.cemconres.2003.10.010](https://doi.org/10.1016/j.cemconres.2003.10.010).
- [23] B. Kerkhoff, E. Siebel, Properties of concrete with recycled aggregates, *Beton.* 2 (2001) 105–108.
- [24] G.-F. Peng, Y.-Z. Huang, H.-S. Wang, J.-F. Zhang, Q.-B. Liu, Mechanical properties of recycled aggregate concrete at low and high water/binder ratios, *Adv. Mater. Sci. Eng.* 2013 (2013).
- [25] C. Hwang, Durability design and performance of self-consolidating lightweight concrete, *19* (2005) 619–626. doi:[10.1016/j.conbuildmat.2005.01.003](https://doi.org/10.1016/j.conbuildmat.2005.01.003).
- [26] BS 12:1989, Specification for ordinary and rapid-hardening Portland cement, Br. Stand. London, UK. (n.d.).
- [27] ASTM C618, Standard Specification for Coal Fly Ash and Raw or Calcined Natural Pozzolan for Use in Concrete, *Am. Soc. Test. Mater.* (2008).
- [28] ASTM C1202, Standard Test Method for Electrical Indication of Concrete’s Ability to Resist Chloride Ion Penetration, (2017).
- [29] ASTM C1585, Standard Test Method for Measurement of Rate of Absorption of Water by Hydraulic-Cement Concretes, (2013).
- [30] ASTM C143 / C143M - 15a, Standard Test Method for Slump of Hydraulic-Cement Concrete, (2015). www.astm.org.
- [31] ASTM C138 / C138M-17a, Standard Test Method for Density (Unit Weight), Yield, and

- Air Content (Gravimetric) of Concrete, (2017). www.astm.org.
- [32] ASTM C191-19, Standard Test Methods for Time of Setting of Hydraulic Cement by Vicat Needle, (2019).
- [33] ASTM C39 / C39M-20, Standard Test Method for Compressive Strength of Cylindrical Concrete Specimens, (2020). www.astm.org.
- [34] ASTM C496 / C496M-17, Standard Test Method for Splitting Tensile Strength of Cylindrical Concrete Specimens, (2017). www.astm.org.
- [35] J. Wang, M. Mu, Y. Liu, Recycled cement, *Constr. Build. Mater.* 190 (2018) 1124–1132.
- [36] J. Xie, J. Wang, R. Rao, C. Wang, C. Fang, Effects of combined usage of GGBS and fly ash on workability and mechanical properties of alkali activated geopolymer concrete with recycled aggregate, *Compos. Part B Eng.* 164 (2019) 179–190.
- [37] S.C. Kou, C.S. Poon, F. Agrela, Comparisons of natural and recycled aggregate concretes prepared with the addition of different mineral admixtures, *Cem. Concr. Compos.* 33 (2011) 788–795. doi:10.1016/j.cemconcomp.2011.05.009.
- [38] S. Elshafie, M. Boulbibane, G. Whittleston, Influence of mineral admixtures on the mechanical properties of fresh and hardened concrete, *Constr. Sci.* 19 (2016) 4–12.
- [39] S.C. Kou, C.S. Poon, Properties of self-compacting concrete prepared with coarse and fine recycled concrete aggregates, *Cem. Concr. Compos.* 31 (2009) 622–627. doi:<https://doi.org/10.1016/j.cemconcomp.2009.06.005>.
- [40] S.J. Barnett, M.N. Soutsos, S.G. Millard, J.H. Bungey, Strength development of mortars containing ground granulated blast-furnace slag: Effect of curing temperature and determination of apparent activation energies, *Cem. Concr. Res.* 36 (2006) 434–440.
- [41] E. Güneyisi, M. Gesoğlu, A study on durability properties of high-performance concretes incorporating high replacement levels of slag, *Mater. Struct.* 41 (2008) 479–493.
- [42] V.B.R. Suda, P.S. Rao, Experimental investigation on optimum usage of Micro silica and GGBS for the strength characteristics of concrete, *Mater. Today Proc.* (2020).
- [43] R.K.D. OBE, J. de Brito, R. V Silva, C.Q. Lye, *Sustainable Construction Materials: Recycled Aggregates*, Woodhead Publishing, 2019.
- [44] D.S. Seo, H.B. Choi, Effects of the old cement mortar attached to the recycled aggregate surface on the bond characteristics between aggregate and cement mortar, *Constr. Build. Mater.* 59 (2014) 72–77.

- [45] C. Li, M. Zhao, F. Ren, N. Liang, J. Li, M. Zhao, Bond Behaviors Between Full-Recycled-Aggregate Concrete and Deformed Steel-Bar, *Open Civ. Eng. J.* 11 (2017).
- [46] M. Etxeberria, E. Vázquez, A. Marí, M. Barra, Influence of amount of recycled coarse aggregates and production process on properties of recycled aggregate concrete, *Cem. Concr. Res.* 37 (2007) 735–742. doi:10.1016/j.cemconres.2007.02.002.
- [47] P.O. Awoyera, A. Adesina, R. Gobinath, Role of recycling fine materials as filler for improving performance of concrete - a review, *Aust. J. Civ. Eng.* (2019). doi:10.1080/14488353.2019.1626692.
- [48] S. Pradhan, S. Kumar, S. V Barai, Recycled aggregate concrete: Particle Packing Method (PPM) of mix design approach, *Constr. Build. Mater.* 152 (2017) 269–284.
- [49] M.L. Berndt, Properties of sustainable concrete containing fly ash, slag and recycled concrete aggregate, *Constr. Build. Mater.* 23 (2009) 2606–2613. doi:https://doi.org/10.1016/j.conbuildmat.2009.02.011.
- [50] J. Kropp, H.K. Hilsdorf, H. Grube, C. Andrade, L. Nilsson, Chapter 2: Transport mechanisms and definitions, *RILEM Rep.* (1995).
- [51] H. Guo, C. Shi, X. Guan, J. Zhu, Y. Ding, T.-C. Ling, H. Zhang, Y. Wang, Durability of recycled aggregate concrete – A review, *Cem. Concr. Compos.* 89 (2018) 251–259. doi:https://doi.org/10.1016/j.cemconcomp.2018.03.008.
- [52] H. Sun, P.M. Wang, J.Y. Sun, Study on the gas anti permeability and carbonation resistance of recycled concrete, *J. Build. Mater.* 9 (2006) 91–96.
- [53] X. Zhang, K. Wu, Mechanism and Key Technique of Mineral Admixture, *JOURNAL-TONGJI Univ.* 32 (2004) 494–498.
- [54] P. Awoyera, A. Adesina, A critical review on application of alkali activated slag as a sustainable composite binder, *Case Stud. Constr. Mater.* (2019) e00268. doi:https://doi.org/10.1016/j.cscm.2019.e00268.
- [55] E. Anastasiou, K.G. Filikas, M. Stefanidou, Utilization of fine recycled aggregates in concrete with fly ash and steel slag, *Constr. Build. Mater.* 50 (2014) 154–161.
- [56] P. Dinakar, K.G. Babu, M. Santhanam, Durability properties of high volume fly ash self compacting concretes, *Cem. Concr. Compos.* 30 (2008) 880–886.
- [57] H. Yiğiter, H. Yazıcı, S. Aydın, Effects of cement type, water/cement ratio and cement content on sea water resistance of concrete, *Build. Environ.* 42 (2007) 1770–1776.

- [58] W. Dodds, C. Goodier, C. Christodoulou, S.A. Austin, D. Dunne, M. Fitt, P. Snowden, Durability performance of structural concrete made with coarse recycled concrete aggregates, in: Proc. Fib Symp. 2016, Performance-Based Approaches Concr. Struct. Cape Town, South Africa, 2016.
- [59] W. Hu, S. Li, C. Song, Z. Chen, L. Chen, Y. Yang, W. Luo, A Laboratory Analysis of Chloride Ions Penetration in Recycled Aggregates Concrete Admixed with Ground Granulated Blast Furnace Slag, in: IOP Conf. Ser. Mater. Sci. Eng., IOP Publishing, 2019: p. 12051.
- [60] C. Faella, C. Lima, E. Martinelli, M. Pepe, R. Realfonzo, Mechanical and durability performance of sustainable structural concretes: An experimental study, *Cem. Concr. Compos.* 71 (2016) 85–96. doi:10.1016/j.cemconcomp.2016.05.009.
- [61] S.-C. Kou, C. Poon, Long-term mechanical and durability properties of recycled aggregate concrete prepared with the incorporation of fly ash, *Cem. Concr. Compos.* 37 (2013) 12–19.
- [62] K. Kapoor, S.P. Singh, B. Singh, Durability of self-compacting concrete made with Recycled Concrete Aggregates and mineral admixtures, *Constr. Build. Mater.* 128 (2016) 67–76. doi:<https://doi.org/10.1016/j.conbuildmat.2016.10.026>.
- [63] W. Chalee, C. Jaturapitakkul, Effects of W/B ratios and fly ash finenesses on chloride diffusion coefficient of concrete in marine environment, *Mater. Struct.* 42 (2009) 505–514.